British Journal of Pharmacology (2009), 156, 1124–1135

0007-1188/09
www.brjpharmacol.org

RESEARCH PAPER

Atypical $P2X_7$ receptor pharmacology in two human osteoblast-like cell lines

SM Alqallaf[1,2], BAJ Evans[2] and EJ Kidd[1]

[1]*Welsh School of Pharmacy, Cardiff University, Cardiff, UK, and* [2]*Department of Child Health, School of Medicine, Cardiff University, Cardiff, UK*

Background and purpose: The expression and function of $P2X_7$ receptors in osteoclasts is well established, but less is known about their role in osteoblast-like cells. A study in $P2X_7$ receptor knockout mice suggested the involvement of these receptors in bone formation. We have investigated the expression and pharmacology of several P2X receptors in two human osteosarcoma cell lines to see if they could be involved in bone turnover in man.
Experimental approach: Reverse transcriptase-polymerase chain reaction and Western blotting were used to study $P2X_2$, $P2X_4$ and $P2X_7$ receptor expression at mRNA and protein levels, respectively, in human osteoblast-like cells. $P2X_7$ receptor pharmacology was studied by measuring pore formation in the presence of different agonists and antagonists using the YO-PRO 1 uptake method.
Key results: $P2X_4$ and $P2X_7$ receptor mRNA and protein were found to be expressed by these cell lines. No evidence was found for $P2X_4$/$P2X_7$ receptor heteropolymerization. 2′-3′-O-(4-benzoylbenzoyl)adenosine 5′-triphosphate (DBzATP) was equipotent to ATP and the antagonists used were either ineffective or weakly blocked pore formation.
Conclusions and implications: This study demonstrates that $P2X_4$ and $P2X_7$ receptors are expressed by human osteoblast-like cells. The affinities of the different agonists suggest that the $P2X_7$ receptor is mainly responsible for pore formation although $P2X_4$ receptors may also be involved. The low affinity of DBzATP and the weak action of the antagonists support the previously described atypical pharmacology of the $P2X_7$ receptor in osteoblasts. Targeting the $P2X_7$ receptor in osteoblasts could represent a promising new treatment for bone diseases such as osteoporosis and rheumatoid arthritis.
British Journal of Pharmacology (2009) **156**, 1124–1135; doi:10.1111/j.1476-5381.2009.00119.x; published online 18 February 2009

Keywords: $P2X_7$ receptor; human osteoblast-like cells; pore formation; YO-PRO 1; ATP; DBzATP; MG63 cells; SaOS2 cells

Abbreviations: AMV, avian myeoloblastosis virus; ATPγS, adenosine-5′-(3-thiotriphosphate); BBG, brilliant blue G; bp, base pairs; DBzATP, 2′-3′-O-(4-benzoylbenzoyl)adenosine 5′-triphosphate; EDTA, ethylenediamine tetraacetic acid; KN-62, 4-[(2S)-2-[(5-isoquinolinylsulphonyl)methylamino]-3-oxo-3-(4-phenyl-1-piperazinyl)propyl] phenyl isoquinolinesulphonic acid ester; oATP, adenosine 5′-triphosphate, periodate oxidized, sodium salt; PBS, phosphate-buffered saline; PPADS, pyridoxal phosphate-6-azo(benzene-2,4-disulphonic acid) tetrasodium salt; YO-PRO 1, quinolinium 4-[(3-methyl-2(3H)-benzoxazolylidene)methyl]-1-[3-(trimethylammonio) propyl]-diiodide

Introduction

ATP can activate two receptor types, ligand-gated ion channel P2X receptors and G protein-coupled P2Y receptors (Suprenant *et al.*, 1996; North and Barnard, 1997); nomenclature follows (Alexander *et al.*, 2008). The $P2X_7$ receptor is the largest (595 amino acids) member of the P2X receptor family (Suprenant *et al.*, 1996; North and Barnard, 1997). It also has the longest C-terminus (242 amino acids) of the P2X family of receptors (Khakh, 2001a).

Correspondence: Dr EJ Kidd, Welsh School of Pharmacy, Cardiff University, Redwood Building, King Edward VII Avenue, Cardiff CF10 3NB, UK. E-mail: KiddEJ@cf.ac.uk
Received 21 August 2008; accepted 18 November 2008

A distinguishing characteristic of the $P2X_7$ receptor is the formation, upon prolonged stimulation, of a non-selective pore in the cell membrane permeable to molecules as large as 900 Daltons, such as ethidium bromide and quinolinium 4-[(3-methyl-2(3H)-benzoxazolylidene)methyl]-1-[3-(trimethylammonio) propyl]-diiodide (YO-PRO 1) (Steinberg *et al.* 1987; Chessell *et al.* 1997; Virginio *et al.* 1999; Hibell *et al.*, 2000). It is believed that pore formation involves the long C-terminus of the $P2X_7$ receptor (Suprenant *et al.*, 1996). However, $P2X_2$ and $P2X_4$ receptors, which have shorter C-termini, can still form pores (Khakh, 2001a; Vial *et al.*, 2004). North, (2002) suggested two mechanisms for the progressive permeability of the $P2X_7$ receptor to cations and larger molecules on activation, the dilation hypothesis and the extra protein hypothesis. An additional characteristic of

the $P2X_7$ receptor is its very low affinity for ATP compared with other P2X receptors (EC_{50} value 300 μM; North and Barnard, 1997). Furthermore, 2′-3′-O-(4-benzoylbenzoyl) adenosine 5′-triphosphate (DBzATP) was claimed to be the most potent agonist by some studies (Chessell *et al.*, 1998; Michel *et al.*, 1999; Lee *et al.*, 2006a), although most of these studies were performed in transfected cells.

$P2X_7$ receptors were initially found in haemopoietic cells, but have since also been identified in other cells such as blood, microglia, brain, nerves, epithelial, lung and spleen cells (Suprenant *et al.*, 1996; Collo *et al.*, 1997; Deuchars *et al.*, 2001; Di Virgilio *et al.*, 2001; North, 2002; Kobayashi *et al.*, 2005). The receptor is also expressed in many pathological conditions such as leukaemia (Thunberg *et al.*, 2002; Wiley *et al.*, 2002; Zhang *et al.*, 2004), intestinal epithelial carcinoma (Coutinho-Silva *et al.*, 2005), cervical cancer (Wang *et al.*, 2004a; 2005) and systemic lupus erythematosus (Elliott *et al.*, 2005). It is thought to be involved in intercellular communication (Chiozzi *et al.*, 1997) and has also been described as a death receptor, because cell death by either necrosis or apoptosis resulting from its stimulation has been reported in many cells (Di Virgilio *et al.*, 1998; Sluyter and Wiley, 2002; Wang *et al.*, 2004b; Elliott *et al.*, 2005). In addition, it was found to be important in immune and inflammatory responses such as cytokine release (Ferrari *et al.*, 1997; Di Virgilio *et al.*, 2001; Solle *et al.*, 2001; Labasi *et al.*, 2002; Bulanova *et al.*, 2005). Additionally, $P2X_7$ receptors were found to be involved in the release of the anti-inflammatory protein, intracellular interleukin-1 receptor antagonist type-1, which can potentially change receptor expression (Wilson *et al.*, 2004).

In bone, many studies have confirmed the expression of $P2X_7$ receptors by osteoclasts and their function in osteoclasts has been clearly described (Hoebertz *et al.*, 2000; 2003; Naemsch *et al.*, 2001). The involvement of $P2X_7$ receptors in the process of calcium signalling between osteoblasts and osteoclasts has also been documented (Jorgensen *et al.*, 2002). (Gartland *et al.*, 2003) reported that blockade of the receptor prevented the formation of multinucleated osteoclasts from human peripheral blood, increased osteoclast apoptosis and eventually inhibited osteoclastic resorption. Ke *et al.* (2003) found that deletion of the $P2X_7$ receptor in mice caused increased resorption proving the significance of the receptor in osteoclast function. However, they also found that multinucleated osteoclasts can be produced even in the absence of the $P2X_7$ receptor.

Less is known about $P2X_7$ receptor expression and function in osteoblasts. Nakamura *et al.* (2000) showed expression of $P2X_7$ receptors by human osteoblast-like MG63 cells at the mRNA level. Gartland *et al.* (2001) demonstrated the expression of $P2X_7$ receptors by two human osteosarcoma cell lines (SaOS2 and Te85) and primary human bone-derived cells using reverse transcriptase-polymerase chain reaction (RT-PCR). They also showed high levels of the receptor protein were found in the SaOS2, but not in the Te85 cells, and varying levels in the primary human cells. $P2X_7$ receptor pore formation was shown in SaOS2 cells, but not in Te85 cells. In SaOS2 and human primary cells, receptor activation caused pore formation, and changes in cell morphology which eventually led to apoptosis. As pore formation in osteoblasts needed 60 min incubation with agonist, while only 5 min is usually needed for haemopoietic cells, the authors suggested an atypical pharmacology of the receptor in these cells (Gartland *et al.*, 2001). The importance of $P2X_7$ receptors in bone formation was established in the study by Ke *et al.* (2003). They compared $P2X_7$ receptor expression and function in osteoblasts from knockout and wild-type mice using RT-PCR and pore formation studies, and found that the knockout mice had reduced bone formation. As $P2X_7$ receptors appear to be involved in bone formation, more information is needed about their expression and pharmacology in osteoblasts. Our study therefore aimed to characterize these receptors more fully in two human osteoblast-like cell lines, MG63 and SaOS2, which are at different stages of development of the osteoblast phenotype (Arnett and Henderson, 1998). SaOS2 cells are believed to be the closest to the mature osteoblast (Hughes and Aubin, 1998). Our results showed that functional $P2X_7$ receptors are expressed by both MG63 and SaOS2 cells. The receptors had an atypical pharmacology as DBzATP was equipotent to ATP. We also showed expression of $P2X_4$ receptors in both cell lines, but our data suggest that it is the $P2X_7$ receptor that is responsible for pore formation.

Methods

Cell culture

MG63 and SaOS2 osteosarcoma cell lines (The European Collection of Cell Cultures, Salisbury, Wiltshire, UK) were grown in 25 cm^2 flasks in Dulbecco's Modified Eagle's Medium (Cambrex, Berks, UK) containing 2 $mmol \cdot L^{-1}$ glutamine and 4500 $mg \cdot L^{-1}$ glucose and supplemented with 5% foetal calf serum (Invitrogen, Paisley, UK). The cells were grown at 37°C in a humidified atmosphere with 5% CO_2 in air, and the medium was changed every 3 or 4 days. Cells were passaged using trypsin-EDTA (0.025% trypsin Worthington Biochemical Corporation, Reading, UK; 0.025% EDTA (ethylenediamine tetraacetic acid)).

RT-PCR

The human $P2X_2$ receptor gene primers (5′–3′) used were: sense – CCCAAATTCCACTTCTCCAA and antisense – GTC CAGGTCACAGTCCCAGT. The human $P2X_4$ receptor gene primers (5′–3′) used were: sense – ACCGTGCTGTGTGACAT CAT and antisense – TGAGTGCTTGTGGAGTGGAG. The human $P2X_7$ receptor gene primers (5′–3′) used were: sense – GTTCCTCTGACCGAGGTT and antisense – CAGGTCTTCTG GTTCCCT. All primers were obtained from Invitrogen and were checked against GenBank for selectivity.

RNA was extracted from cells using the MIDAS RNA extraction kit (Biogene, Cambridge, UK) according to the manufacturer's instructions, and treated with DNase (Ambion, Warrington, UK). RT reactions were carried out to prepare cDNA from 1 μg RNA using avian myeloblastosis virus (AMV) RT according to the manufacturer's instructions (Promega, Southampton, UK). Reactions were performed in parallel without the RT enzyme. cDNA samples were stored at –20°C until needed. PCR reactions (25 μL) were performed using 1 μL of the RT reaction or water and 10 pmol of each

primer. All PCR reactions were run in a Perkin Elmer 480 Thermal Cycler as follows: 94°C for 3 min, 60°C for 1 min, 72°C for 1 min and then 35 cycles at: 94°C for 30 s, 60°C for 1 min, 72°C for 1 min. PCR samples and marker (0.3 μg·lane^{-1}, New England Biolabs, Herts, UK) were then separated in 1.5% agarose gels containing 1.27 μmol·L^{-1} ethidium bromide using TBE buffer (90 mmol·L^{-1} Tris base, 90 mmol·L^{-1} boric acid, 2.5 mmol·L^{-1} EDTA). The bands were visualized with a UV-transilluminator (Fotodyne Incorporated, New Berlin, WI, USA), and photographed using a Polaroid camera. The bands obtained were excised from the gels, incubated in 50 μL sterile water, kept at 4°C for 48 h and the cDNA eluted into the water and sequenced using the Big Dye® Terminator V 3.1 Cycle Sequencing kit (Applied Biosystems, Warrington, UK).

Receptor deglycosylation

Deglycosylation of the $P2X_7$ receptor in MG63 and SaOS2 cell membranes obtained as described previously (Yates *et al.*, 2006) was studied using a Glycoprotein Deglycosylation Kit (Calbiochem, Nottingham, UK). According to the manufacturer's instructions, samples were centrifuged at 15 306 g at 4°C for 15 min, and the pellet resuspended in 30 μL deionized water. Half the sample was incubated with a total of 2.5 U of the enzymes (N-glycosidase F, α2-3,6,8,9-Neuroaminidase and Endo-α-N-acetylgalactosminidase), while the other half was incubated with distilled water. Both samples were incubated for 3 h at 37°C and the reaction was then stopped with 3X Laemmli sample buffer (0.19 mol·L^{-1} Tris base, 12% SDS, 30% glycerol, 15% β-mercaptoethanol, 1 mg·mL^{-1} bromophenol blue) and they were then stored at –20°C until use.

Western blotting

Cell lysis was performed as described previously (Thomas *et al.*, 2006). Cell nuclei were isolated using lysis buffer (10 mmol·L^{-1} Tris base, 10 mmol·L^{-1} NaCl, 5 mmol·L^{-1} $MgCl_2$, 0.5% Nonidet P 40, pH 7.4), the lysed cells were centrifuged at 400 g at 4°C for 5 min and the pellet was resuspended in 4 mL lysis buffer, vortexed and centrifuged as above. Protein concentrations were determined using the bicinchonic acid method (Perbio Science UK Ltd., Cramlington, UK)

Western blotting was performed using standard methods (Thomas *et al.*, 2006). Membrane samples of human embryonic kidney cells (HEK393) transfected with the $P2X_7$ receptor (HEK7) were used as a positive control (Michel *et al.*, 1999). The samples and molecular weight marker (Precision Plus Protein Standards marker, Bio-Rad Laboratories, Hertfordshire, UK) were loaded onto 10% polyacrylamide gels and separated by sodium dodecyl sulphate-polyacrylamide gel electrophoresis in running buffer (25 mmol·L^{-1} Tris base, 190 mmol·L^{-1} glycine, 0.05% SDS, pH 8.3). The separated proteins were then blotted on to 0.2 μm nitrocellulose membranes (GE, Little Chalfont, UK), washed in Tris-buffered saline with Tween 20 (TBST, 2 mmol·L^{-1} Tris, 15 mmol·L^{-1} NaCl, 0.1% Tween-20, pH 7.5) and blocked for 1 h, at room temperature, in TBST supplemented with 5% w·v^{-1} fat-free dried milk (BLOTTO; Marvel, Premier International Ltd., Spalding, UK). The membranes were then incubated with the relevant primary antibody in 1% BLOTTO at 4°C overnight. For re-adsorption of the anti-$P2X_7$ receptor antibody with its corresponding peptide, 1.2 μg of peptide was incubated at 4°C overnight with the $rP2X_7$ antibody in 1% w·v^{-1} BLOTTO before use. Re-adsorption of the anti-$P2X_2$ and anti-$P2X_4$ receptor antibodies with 4 and 3.2 μg of their corresponding peptides, respectively, was also performed. Membranes were washed five times in TBST and incubated with anti-rabbit horseradish peroxidase-conjugated secondary antibody (1:20 000, Vector Laboratories, Peterborough, UK) for 1 h at RT. The membranes were washed as above in TBST, the bands visualized using enhanced chemiluminiscent detection (Super Signal®, West Dura, Perbio Science), and exposed to high performance chemiluminescent X-ray film (GE).

Immunocytochemistry

Immunocytochemistry was performed as described previously (Thomas *et al.*, 2006) with several modifications as detailed below. Both cell lines were grown on 13 mm coverslips treated with 2% 3-aminopropyltriethoxy silane in acetone in 24 well cluster plates in the appropriate growth media. Cells were fixed in 2% formaldehyde in 0.1 mol·L^{-1} phosphate-buffered saline (PBS, 145 mmol·L^{-1} NaCl, 96.4 mmol·L^{-1} $NaHPO_4$, 21.5 mmol·L^{-1} NaH_2PO_4), pH 7.4, for 15 min at room temperature and subsequently washed three times in PBS (each 5 min). Coverslips were blocked for 30 min in 3% goat serum, 1% bovine serum albumin and 0.1% Triton X-100 in PBS. The coverslips were incubated with $rP2X_7$ receptor primary antibody (1:1000) in blocking buffer for 24–72 h at 4°C. To confirm the labelling seen, the $rP2X_7$ receptor antibody was pre-adsorbed for 48 h in blocking solution with 0.8 μg of its corresponding peptide. After washing as above, coverslips were then incubated with an anti-rabbit secondary antibody conjugated to Cy3 (Millipore, Watford, UK), 1:800, for 1 h at room temperature in the dark. The coverslips were washed as above and finally dipped in distilled water to remove any residual buffer salts before being left to dry in the dark. Coverslips were mounted on ethanol-rinsed slides using an anti-fade agent (fluorescent mounting medium, DAKO UK Ltd., Ely, UK) and stored at 4°C. Slides were visualized using a Leica DMRA2 microscope (Leica, Wetzlar, Germany), images were recorded using a digital camera (DC 500, Leica) and the Leica FW 4000 software and images were processed using Adobe Photoshop.

YO-PRO 1 Uptake

$P2X_7$ receptor activation was studied using a modified version of the YO-PRO 1 uptake method (Michel *et al.*, 1999). Cells were grown in 25 cm^2 flasks until confluent, and then collected using trypsin/EDTA. The cells were resuspended in 1 mL of growth medium and centrifuged at 179× *g* at room temperature for 5 min. The cell pellet was then resuspended in 10 mL Dulbecco's PBS (Invitrogen), counted and centrifuged again at 200× *g* for 5 min at room temperature. The cell pellet was resuspended in 10 mL ice-cold assay buffer pH 7.4 (5 mmol·L^{-1} KCl, 0.5 mmol·L^{-1} $CaCl_2$, 10 mmol·L^{-1} glucose, 10 mmol·L^{-1} HEPES, 10 mmol·L^{-1} N-methyl-D-glucamine and 280 mmol·L^{-1} sucrose) and centrifuged at 200× *g* for 5 min at room temperature and resuspended again in assay buffer at

37°C. Approximately 100 000 cells per well were added to 96-well black plates (Greiner Bio-One Ltd., Stonehouse, UK) containing buffer or an agonist and 1 μmol·L^{-1} YO-PRO 1 in assay buffer and the plate was incubated at 37°C for various times. YO-PRO 1 fluorescence was monitored in a 96-well plate reader (Fluostar Optima, BMG Labtechnologies Ltd., Aylesbury, UK) using an excitation wavelength of 485 nm and an emission wavelength of 520 nm. To determine the optimum time needed for the pore formation, MG63 and SaOS2 cells were incubated with 0.8 mmol·L^{-1} ATP for different periods (5–30 min) and the uptake was measured. To find the best assay buffer for YO-PRO 1 uptake in MG63 and SaOS2 cells, five different buffers were studied. In addition to the assay buffer above (A), 0.8 mmol·L^{-1} ATP was used to induce YO-PRO 1 uptake in the following buffers: (B) assay buffer containing 0.1 mmol·L^{-1} $CaCl_2$, (C) the same buffer containing 0.1 mmol·L^{-1} EDTA in place of $CaCl_2$ (Michel *et al*., 1999), (D) PBS and (E) a buffer containing 125 mmol·L^{-1} KCl, 1 mmol·L^{-1} EDTA, 5 mmol·L^{-1} glucose and 20 mmol·L^{-1} HEPES, pH 7.4 (Gartland *et al*., 2001). Experiments were also performed to investigate receptor desensitization. Here, flasks of cells were incubated at 37°C for 20 min with or without 3 mmol·L^{-1} ATP and the YO-PRO 1 uptake was then determined.

Different P2X receptor antagonists were studied to investigate whether they could block pore formation induced by ATP and DBzATP. For this purpose, cells were incubated with different concentrations of the antagonists for 1 h in the presence of 1 μmol·L^{-1} YO-PRO 1 in assay buffer at 37°C, then ATP or DBzATP was added and the assay performed.

An experiment was performed to investigate the potential involvement of $P2X_4$ receptors in the YO-PRO 1 uptake. Cells were pre-incubated with 10 μmol·L^{-1} ivermectin for 10 min and then YO-PRO 1 uptake induced by 1 and 0.5 mmol·L^{-1} ATP or DBzATP was measured.

Data expression and statistical analysis

For the YO-PRO 1 uptake studies, data were expressed as % of maximum uptake of each agonist and EC_{50} values were calculated using Prism 4.0 (GraphPad Software, La Jolla, CA, USA).

Results were analysed using one-way ANOVA. Multiple comparisons were then made using Bonferroni or Dunnett's *post hoc* tests in Prism 4.0. *P* values less than 0.05 were considered to be statistically significant. The results were expressed as the mean ± SD.

Drugs, chemicals and antibodies

All chemicals were of Analar grade and were obtained from Sigma (Poole, Dorset, UK) or Fisher (Leicester, UK), unless otherwise stated.

ATP, DBzATP, adenosine-5′-(3-thiotriphosphate) (ATPγS), brilliant blue G (BBG), adenosine 5′-triphosphate, periodate oxidized, sodium salt (oATP) and pyridoxal phosphate-6-azo(benzene-2,4-disulphonic acid) tetrasodium salt (PPADS) were obtained from Sigma and 2-(methylthio)adenosine 5′-triphosphate tetrasodium salt (2-Me-S-ATP) and 4-[(2S)-2-[(5-isoquinolinylsulphonyl)methylamino]-3-oxo-3-(4-phenyl-1-piperazinyl)propyl] phenyl isoquinolinesulphonic acid ester (KN-62) were obtained from Tocris (Bristol, UK).

YO-PRO 1 1 mmol·L^{-1} solution in DMSO was obtained from Invitrogen. Polyclonal rabbit anti-C-terminal $P2X_2$, anti-$P2X_4$, and anti-$P2X_7$ receptor antibodies and their corresponding peptides were obtained from Alomone Labs, Jerusalem, Israel and are referred to as $rP2X_2$, $rP2X_4$ and $rP2X_7$ antibodies respectively.

Results

RT-PCR

Reverse transcriptase-polymerase chain reaction for $P2X_4$ (Figure 1B) and $P2X_7$ receptor mRNA (Figure 1C), using MG63 and SAOS2 cell RNA samples gave bands of the expected sizes [200 base pairs (bp) for the $P2X_4$ and 100 bp for the $P2X_7$ receptor]. No bands were seen in control samples (water or no AMV in the RT reaction) (Figure 1B,C). To confirm these results, sequencing was carried out on the bands excised from the gel and the expected sequence of nucleotides was obtained for each receptor (data not shown). No bands were seen using the $P2X_2$ receptor primers in either cell line (Figure 1A). A human pancreatic cell line, BON-1, was used as

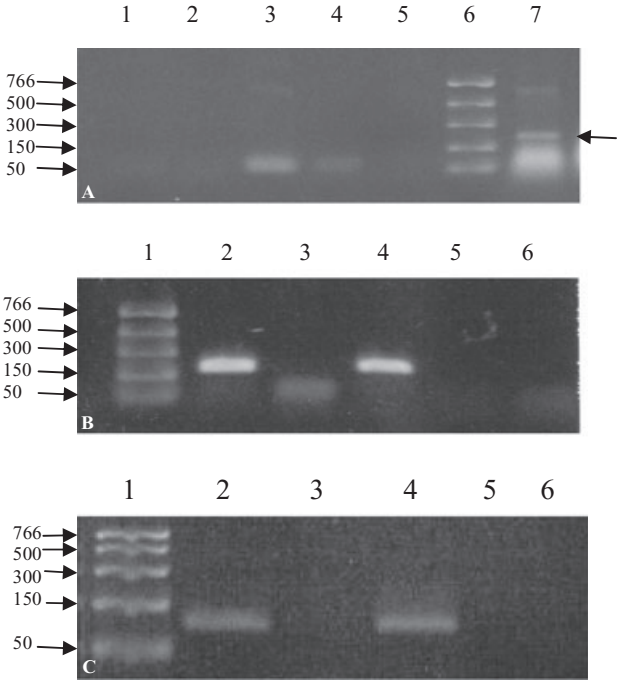

Figure 1 Representative example of RT-PCR for $P2X_2$, $P2X_4$ and $P2X_7$ receptor mRNAs in MG63 and SaOS2 cell samples. RT-PCR was performed on RNA extracted from MG63 and SaOS2 cells using primers for the human $P2X_2$ (A), $P2X_4$ (B) and $P2X_7$ (C) receptors. In (A), no bands were seen for MG63 (lanes 1 and 2) or SaOS2 (lanes 3 and 4) cells in the presence (lanes 1 and 3) or absence (lanes 2 and 4) of the RT enzyme. Human BON-1 pancreatic cell cDNA was used as a positive control (lane 7) and gave the expected band of 200 bp (arrow). The marker ladder is in lane 6. In (B) and (C) bands were seen in lanes 2 and 4 for MG63 and SaOS2 samples, respectively, corresponding to $P2X_4$ (200 bp, B) or $P2X_7$ (100 bp, C) receptors. No bands were seen when MG63 (lane 3) and SaOS2 (lane 5) samples were incubated without the RT enzyme or when sterile water (lane 6) was used in the PCR reaction instead of the RT sample (lane 6). The marker ladder is shown in lane 1. *n* = 2–5. RT-PCR, reverse transcriptase-polymerase chain reaction.

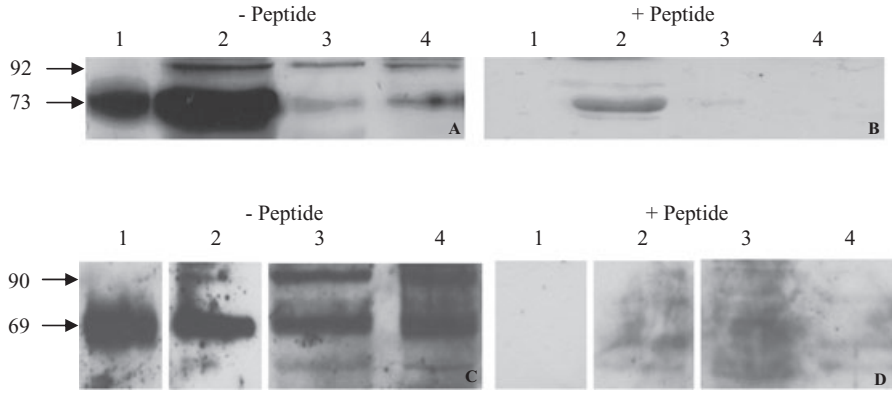

Figure 2 Representative example of Western blotting for $P2X_7$ receptors in SaOS2 and MG63 cells. Positive control (10 μg of HEK7 cell membrane, lane 1), and 25 μg of SaOS2 (A & B) or MG63 (C & D) cell membranes (lane 2), lysate (lane 3) and nuclei (lane 4) were separated on 10% gels and bands detected after prior incubation of the $rP2X_7$ receptor antibody (1:1000) with (B & D) or without (A & C) its corresponding peptide (1.2 μg). Bands were seen at 73 and 92 kDa in SaOS2 cells (A) and at 69 and 90 kDa in MG63 cells (C). All these bands disappeared or were greatly reduced in intensity after preincubation with the peptide (B & D). $n = 10$.

a positive control (Lynch *et al.*, 1999) to demonstrate that the primers did amplify the expected $P2X_2$ receptor product of 200 bp (Figure 1A).

Western blotting

Membranes of HEK7 cells were used as a positive control. Using the $rP2X_7$ receptor antibody, bands were seen in the positive control, SaOS2 and MG63 cell membranes, lysates, and nuclei at 68 ± 5 kDa, and at 89 ± 3 kDa (Figure 2A,C). Bands larger than 100 kDa were also seen in the SaOS2 and MG63 lysate and nuclei samples (data not shown). Following pre-incubation of the $rP2X_7$ receptor antibody with its corresponding peptide, the bands in the HEK7 positive control, SaOS2 and MG63 membranes, lysates and nuclei either disappeared or were greatly reduced in intensity (Figure 2B,D).

Additionally, Western blotting was performed to investigate the expression of the other pore-forming P2X receptors, $P2X_2$ and $P2X_4$, in SaOS2 and MG63 cells. Rat brain membranes were used as a positive control. Using the $rP2X_4$ receptor antibody, bands were seen in the positive control and MG63 and SaOS2 cell lysate samples at 64 ± 1.8 kDa for the $P2X_4$ receptor (Figure 3A). Following pre-incubation of the $rP2X_4$ receptor antibody with its corresponding peptide, all these bands disappeared (Figure 3B). Using the anti-$P2X_2$ receptor antibody, a band at 60 ± 1.8 kDa was seen in all samples but, following pre-incubation of the $rP2X_2$ receptor antibody with its corresponding peptide, only the positive control band disappeared (data not shown).

$P2X_7$ receptor deglycosylation

Deglycosylation of MG63 and SaOS2 cell membranes reduced the apparent molecular mass of the $P2X_7$ receptor from 68 ± 1.7 kDa to 60 ± 25 kDa and from 70 ± 1.9 kDa to 61 ± 2 kDa in MG63 and SaOS2 cells, respectively (Figure 4). The higher molecular mass band (~89 kDa) was not detected in any of these experiments.

$P2X_7$/$P2X_4$ receptor co-immunoprecipitation

$P2X_4$ and $P2X_7$ receptors were immunoprecipitated from MG63 and SaOS2 cell lysates using the $rP2X_4$ and $rP2X_7$ receptor antibodies, respectively. After separation and blotting as described above, membranes were probed with the same antibodies. Immunoprecipitation of both receptors was seen with their corresponding antibodies but no bands

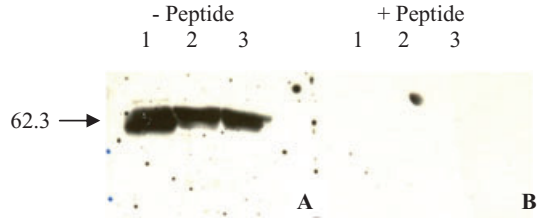

Figure 3 Representative example of Western blotting for $P2X_4$ receptors in SaOS2 and MG63 cells. Positive control (60 μg of rat brain membranes, lane 1), and 12.5 μg of MG63 (lane 2 A and B) and SaOS2 (lane 3 A and B) cell lysates were separated on 10% gels and bands detected after prior incubation of the $rP2X_4$ receptor antibody (1:1000) with (B) or without (A) its corresponding peptide (3.2 μg). A band was seen in all the samples at 62.3 kDa (A), which disappeared after preincubation with the peptide (B). $n = 5$.

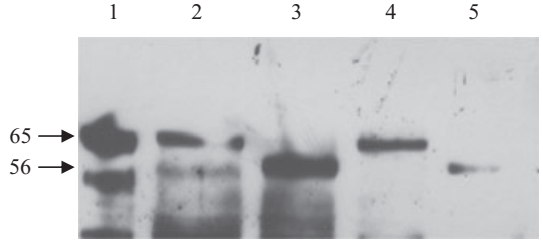

Figure 4 Representative example of Western blotting of the effect of deglycosylation of $P2X_7$ receptors in MG63 and SaOS2 cell membranes. Positive control (5 μg of HEK7 cell membranes, lane 1), 100 μg of glycosylated MG63 (lane 2) and SaOS2 (lane 4) cell membranes, and 100 μg of deglycosylated MG63 (lane 3) and SaOS2 (lane 5) cell membranes were separated on 10% gels and bands detected using the $rP2X_7$ antibody (1:2000). Bands were seen in the positive control at 63.7 kDa, glycosylated MG63 cell membranes at 65.2 kDa, deglycosylated MG63 cell membranes at 56.1 kDa, glycosylated SaOS2 cell membranes at 66.7 kDa and deglycosylated SaOS2 cell membranes at 58.4 kDa. No higher bands were seen in any of the samples. $n = 3$.

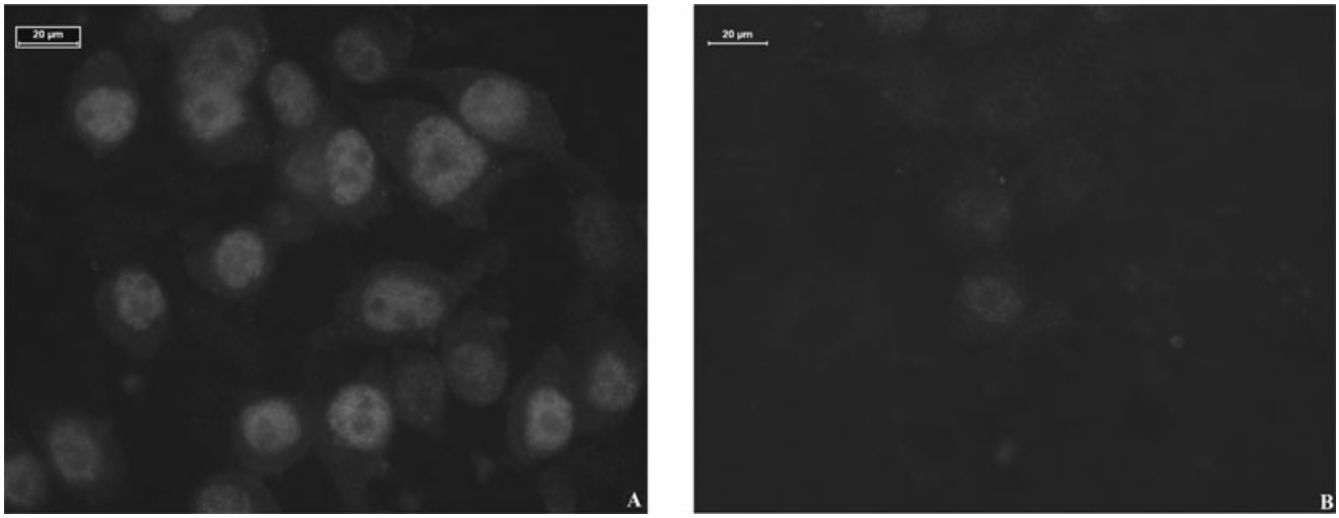

Figure 5 Representative example of immunocytochemistry in MG63 cells. MG63 cells were incubated with the rP2X$_7$ receptor antibody (1:1000) after prior incubation with (B) or without (A) its corresponding peptide (0.8 µg) and detected with an anti-rabbit secondary antibody conjugated to Cy3 (1:800). $n = 3$.

were obtained for the P2X$_7$ receptor co-immuno-precipitated with the rP2X$_4$ receptor antibody or vice versa (data not shown).

Immunocytochemistry

Much more intense labelling of the nuclei compared with the cytoplasm was observed when cells were incubated with the rP2X$_7$ antibody. A representative example of MG63 cells is shown in Figure 5A. No labelling was seen in control cells incubated with the blocking solution in the absence of the antibody (data not shown). To confirm the labelling seen, the rP2X$_7$ receptor antibody was pre-adsorbed with its corresponding peptide and the labelling disappeared or was much weaker (Figure 5B). Similar results were seen with SaOS2 cells (data not shown).

YO-PRO 1 uptake

Initial experiments investigated the optimum assay buffer and incubation period for the agonists in both cell lines. The highest uptake was obtained with assay buffer (A) described by Michel *et al*. (1999) and uptake was also obtained with buffer (B) (data not shown). No uptake above baseline was obtained with buffers (C), (D) or (E) (data not shown). An incubation period of 5 min gave the highest uptake in both cell lines and a significant decrease in uptake was seen after 20 and 30 min incubation in SaOS2 cells (data not shown). YO-PRO 1 uptake was lower than control levels when cells were pre-incubated for 60 min with ATP (data not shown). All subsequent experiments were therefore carried out using assay buffer (A) and 5 min incubation.

Effect of agonists on YO-PRO 1 uptake

All the agonists used, ATP, DBzATP, ATPγS and 2Me-S-ATP, were found to induce YO-PRO 1 uptake in SaOS2 cells with similar potency (Figure 6, Table 1). ATP and DBzATP also induced uptake in MG63 cells with similar potency (Table 1). YO-PRO 1 uptake induced by ATP and 2Me-S-ATP at concentrations higher than 1 mmol·L^{-1} was less than that induced by 1 mmol·L^{-1}. Table 1 compares the EC_{50} values of the agonists used in this study with those reported in the literature for the influx of intracellular calcium in cells transfected with human P2X$_2$, P2X$_4$ and P2X$_7$ receptors. With the exception of the data for DBzATP, EC_{50} values in this study were closer to those for P2X$_7$ receptors than for P2X$_2$ or P2X$_4$ receptors.

Receptor desensitization with ATP in MG63 and SaOS2 cells did not alter the concentration-effect curves for ATP compared with control cells. The EC_{50} values for ATP in the control and treated MG63 cells were 0.44 ± 0.02 mmol·L^{-1} and 0.43 ± 0.07 mmol·L^{-1}, respectively, while in SaOS2 cells, the EC_{50} value for ATP was 0.58 ± 0.05 mmol·L^{-1} in both control and treated cells.

Effect of antagonists on YO-PRO 1 uptake

Figures 7–10 show the concentration-effect curves for ATP in the presence of different concentrations of BBG, KN-62, oATP and PPADS in MG63 (A) and SaOS2 (B) cells. EC_{50} values for ATP and DBzATP were not significantly altered by any of the antagonists. The EC_{50} values for the highest antagonist concentrations used are shown in Table 2. In MG63 cells, 0.2 µmol·L^{-1} BBG significantly increased the uptake induced by 30 and 300 µmol·L^{-1} ATP, but 5 µmol·L^{-1} BBG significantly reduced the maximum YO-PRO 1 uptake induced by ATP by approximately 20% (Figure 7A). BBG had no effect on YO-PRO 1 uptake induced by ATP in SaOS2 cells (Figure 7B). KN-62 did not significantly alter the maximum YO-PRO 1 uptake induced by ATP in MG63 cells (Figure 8A). In SaOS2 cells, 10 µmol·L^{-1} KN-62 significantly reduced the maximum YO-PRO 1 uptake induced by ATP by approximately 11% (Figure 8B). In MG63 cells, 30 and 300 nmol·L^{-1} PPADS significantly decreased the maximum uptake induced by ATP by approximately 11 and 17% respectively (Figure 9A). PPADS did not significantly alter YO-PRO 1 uptake induced by ATP in

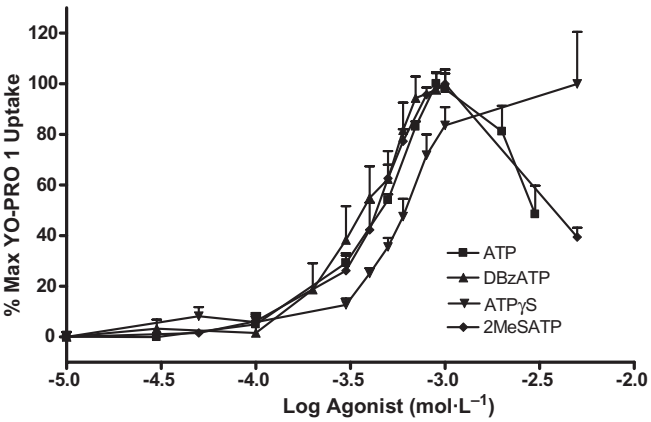

Figure 6 Concentration-effect curves for ATP, DBzATP, ATPγS and 2MeSATP in SaOS2 cells. SaOS2 cells (approximately 100 000 cells per well) were incubated with each agonist and 1 μmol·L^{-1} YO-PRO 1 in 0.5 mmol·L^{-1} $CaCl_2$-containing assay buffer at 37°C for 5 min. YO-PRO 1 fluorescence was monitored in a 96-well plate reader using an excitation wavelength of 485 nm, and an emission wavelength of 520 nm. Data are expressed as % maximum YO-PRO 1 uptake for each agonist. *n* = 3–19. 2MeSATP, 2-(methylthio)adenosine 5′-triphosphate tetrasodium salt; ATPγS, adenosine-5′-(3-thiotriphosphate); DBzATP, 2′-3′-O-(4-benzoylbenzoyl)adenosine 5′-triphosphate; YO-PRO 1, quinolinium 4-[(3-methyl-2(3H)-benzoxazolylidene)methyl]-1-[3-(trimethylammonio) propyl]-diiodide.

Table 1 Comparison of EC_{50} values (μmol·L^{-1} ± SD) for ATP, DBzATP, ATPγS and 2MeSATP obtained here with literature values (μmol·L^{-1}) for human $P2X_2$, $P2X_4$ and $P2X_7$ receptors

Agonist	*MG63*[a]	*SaOS2*[a]	*hP2X2*[b]	*hP2X4*[c]	*hP2X7*[c]
ATP	360 ± 100	430 ± 200	1	0.48	95
DBzATP	500 ± 100	360 ± 200	0.42	0.49	4.7
ATPγS	ND	600 ± 100	1.35	11	>100
2MeSATP	ND	420 ± 100	0.81	2.2	>100

[a]EC_{50} values (μmol·L^{-1} ± SD) obtained in this study for MG63 and SaOS2 cells.
[b]EC_{50} values (μmol·L^{-1}) for the influx of intracellular calcium measured in human astrocytoma cells transfected with human $P2X_2$ ($hP2X_2$) receptors (Lynch *et al.*, 1999).
[c]EC_{50} values (μmol·L^{-1}) for the influx of intracellular calcium measured in human astrocytoma cells transfected with human $P2X_4$ ($hP2X_4$) or human $P2X_7$ ($hP2X_7$) receptors (Bianchi *et al.*, 1999).
2MeSATP, 2-(methylthio)adenosine 5′-triphosphate tetrasodium salt; ATPγS, adenosine-5′-(3-thiotriphosphate); DBzATP, 2′-3′-O-(4-benzoylbenzoyl) adenosine 5′-triphosphate; ND, not determined.

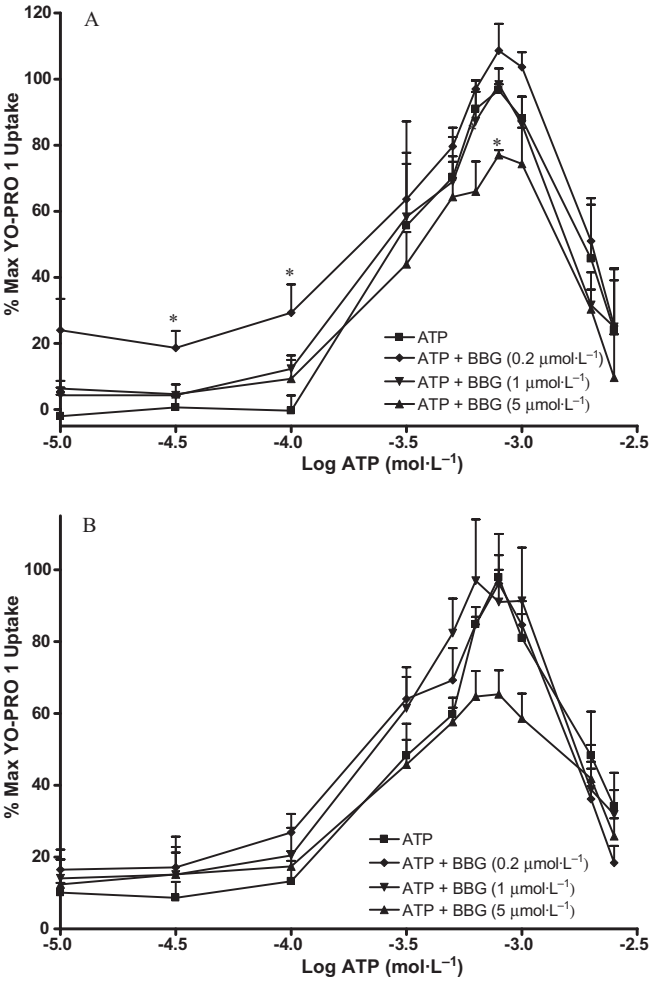

Figure 7 ATP concentration-effect curves in MG63 and SaOS2 cells in the presence of BBG. MG63 (A) or SaOS2 (B) cells (approximately 100 000 cells per well) were incubated with 1 μmol·L^{-1} YO-PRO 1 in assay buffer in the presence of water (vehicle for BBG), or 0.2 μmol·L^{-1}, 1 μmol·L^{-1}, or 5 μmol·L^{-1} BBG at 37°C for 1 h followed by ATP for 5 min. YO-PRO 1 fluorescence was monitored in a 96-well plate reader using an excitation wavelength of 485 nm, and an emission wavelength of 520 nm. Data are expressed as % of maximum uptake of ATP in the presence of the vehicle. Statistical analyses were performed using one-way ANOVA with Bonferroni *post hoc* test. *P < 0.05 versus control. *n* = 3–4. BBG, brilliant blue G; YO-PRO 1, quinolinium 4-[(3-methyl-2(3H)-benzoxazolylidene) methyl]-1-[3-(trimethylammonio) propyl]-diiodide.

SaOS2 cells (Figure 9B). oATP had no significant effect on ATP-induced YO-PRO 1 uptake in MG63 (Figure 10A) or SaOS2 (Figure 10B) cells.

YO-PRO 1 uptake induced by DBzATP in SaOS2 cells was not significantly altered by BBG or KN-62 (Table 2).

Effect of ivermectin on YO-PRO 1 uptake

Ivermectin had no significant effect on the uptake of YO-PRO 1 induced by ATP or DBzATP in MG63 or SaOS2 cells. In MG63 cells 1 mmol·L^{-1} ATP increased YO-PRO 1 uptake by 82 ± 16% compared with control, while in the presence of ivermectin the increase was 73 ± 14%. 1 mmol·L^{-1} DBzATP increased YO-PRO 1 uptake by 99 ± 14% compared with control, while in the presence of ivermectin the increase was 98 ± 13%. In SaOS2 cells, 1mM ATP increased YO-PRO 1 uptake by 65 ± 19% compared with control, while in the presence of ivermectin the increase was 67 ± 14%. 1 mmol·L^{-1} DBzATP increased YO-PRO 1 uptake by 91 ± 14% compared with control, while in the presence of ivermectin the increase was 89 ± 13%.

Discussion

Reverse transcriptase-polymerase chain reaction was utilized to investigate the expression of $P2X_2$, $P2X_4$ and $P2X_7$ receptors at the mRNA level in both cell lines. Both $P2X_4$ and $P2X_7$

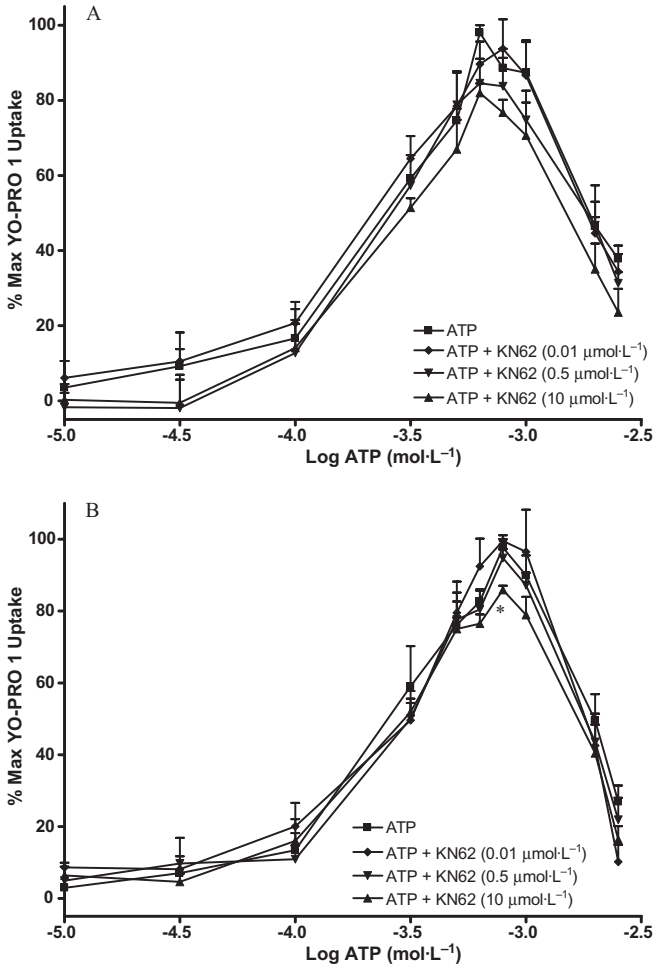

Figure 8 ATP concentration-effect curves in MG63 and SaOS2 cells in the presence of KN-62. MG63 (A) or SaOS2 (B) cells (approximately 100 000 cells per well) were incubated with 1 μmol·L^{-1} YO-PRO 1 in assay buffer in the presence of DMSO (vehicle for KN-62), 0.01 μmol·L^{-1}, 0.5 μmol·L^{-1}, or 10 μmol·L^{-1} KN-62 at 37°C for 1 h followed by ATP for 5 min. YO-PRO 1 fluorescence was monitored in a 96-well plate reader using an excitation wavelength of 485 nm, and an emission wavelength of 520 nm. Data are expressed as % of maximum uptake of ATP in the presence of the vehicle. Statistical analyses were performed using one-way ANOVA with Bonferroni *post hoc* test. **P* < 0.05 versus control. *n* = 3. KN-62, 4-[(2S)-2-[(5-isoquinolinylsulphonyl)methylamino]-3-oxo-3-(4-phenyl-1-piperazinyl)propyl] phenyl isoquinolinesulphonic acid ester; YO-PRO 1, quinolinium 4-[(3-methyl-2(3H)-benzoxazolylidene) methyl]-1-[3-(trimethylammonio) propyl]-diiodide.

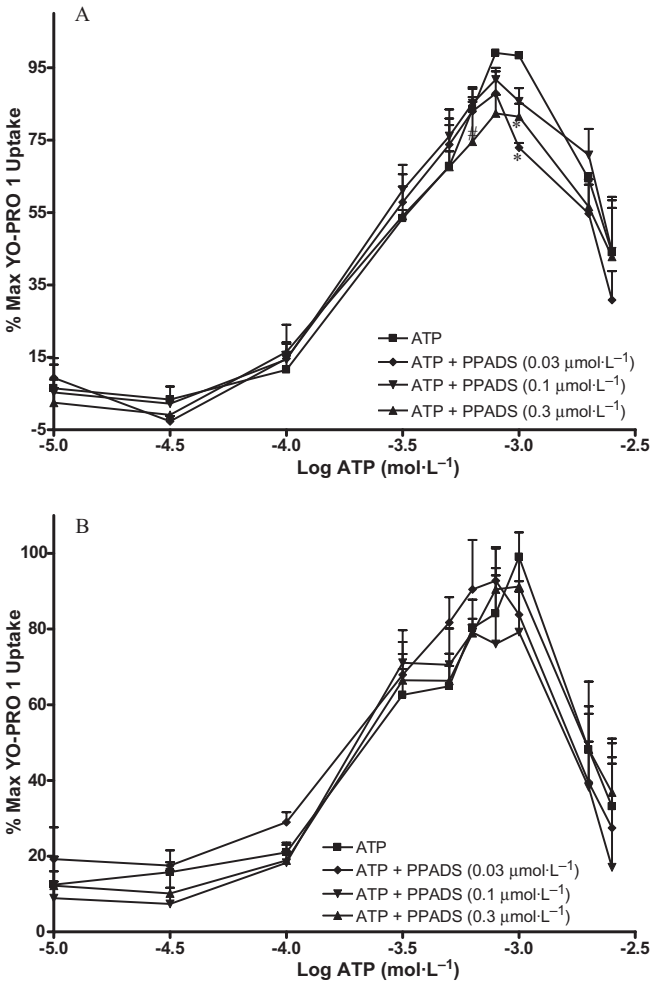

Figure 9 ATP concentration-effect curves in MG63 and SaOS2 cells in the presence of PPADS. MG63 (A) or SaOS2 (B) cells (approximately 100 000 cells per well) were incubated with 1 μmol·L^{-1} YO-PRO 1 in assay buffer in the presence of water (vehicle for PPADS), 0.03 μmol·L^{-1}, 0.1 μmol·L^{-1}, or 0.3 μmol·L^{-1} PPADS at 37°C for 1 h followed by ATP for 5 min. YO-PRO 1 fluorescence was monitored in a 96-well plate reader using an excitation wavelength of 485 nm, and an emission wavelength of 520 nm. Data are expressed as % of maximum uptake of ATP in the presence of the vehicle. Statistical analyses were performed using one-way ANOVA with Bonferroni *post hoc* test. **P* < 0.05 and #*P* < 0.001 versus control. *n* = 3. PPADS, pyridoxal phosphate-6-azo(benzene-2,4-disulphonic acid) tetrasodium salt; YO-PRO 1, quinolinium 4-[(3-methyl-2(3H)-benzoxazolylidene)methyl]-1-[3-(trimethylammonio) propyl]-diiodide.

receptor mRNAs were detected in MG63 and SaOS2 cells and the identity of the DNA bands was confirmed by sequencing for both receptors. P2X$_4$ receptor mRNA has been found previously in MG63 cells (Nakamura *et al.*, 2000) but not in SaOS2 cells. Our data for P2X$_7$ receptor mRNA confirm previous findings for both cell lines (Nakamura *et al.*, 2000; Gartland *et al.*, 2001). P2X$_2$ receptor mRNA was not detected in MG63 or SaOS2 cells suggesting that the receptor is not expressed or present in very low amounts in these cells. The positive control for P2X$_2$ receptor mRNA demonstrated that P2X$_2$ receptor cDNA could be detected with these PCR primers.

Western blotting detected both P2X$_4$ and P2X$_7$ receptors in MG63 and SaOS2 cells confirming the RT-PCR results. The specificity of the labelling for both antibodies was confirmed by the marked reduction in intensity or disappearance of the receptor bands in all samples following pre-adsorption of the primary antibodies with their corresponding peptides. We are not aware of any previous reports describing the expression of the P2X$_4$ receptor protein in osteoblast-like cells so our results are the first demonstration of this receptor in these cells and suggest that P2X$_4$ receptors may have a role in osteoblast functions.

Western blotting detected two bands of approximately 68 and 89 kDa for the P2X$_7$ receptor in both cell lines. The 89 kDa band has been reported in other cells (Wang *et al.*, 2005). They claimed that it was the mature and functional

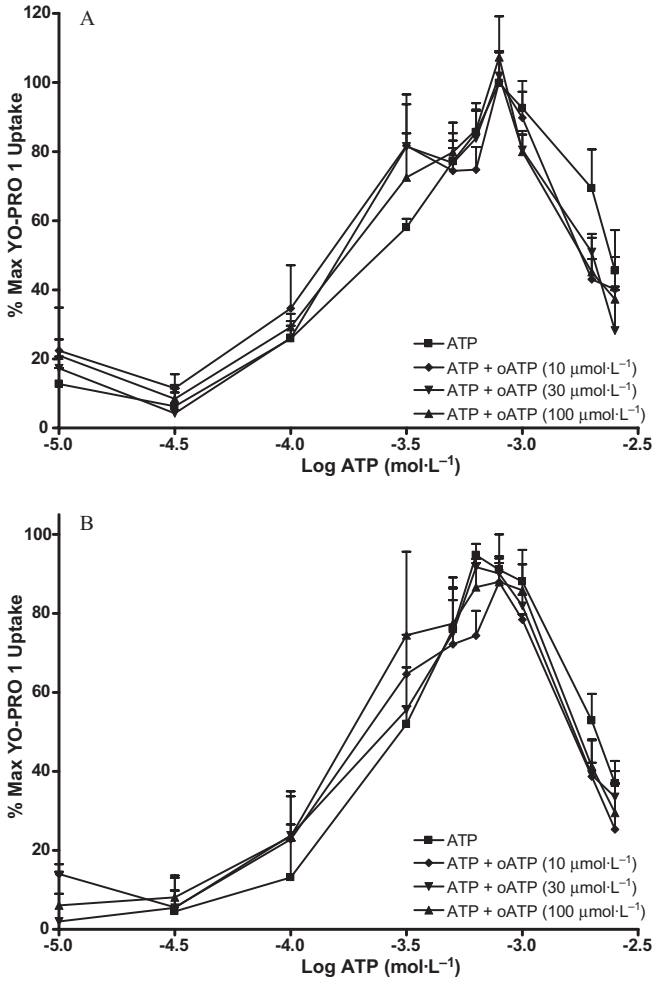

Figure 10 ATP concentration-effect curves in MG63 and SaOS2 cells in the presence of oATP. MG63 (A) or SaOS2 (B) cells (approximately 100 000 cells per well) were incubated with 1 μmol·L^{-1} YO-PRO 1 in assay buffer in the presence of water (vehicle for oATP), 10 μmol·L^{-1}, 30 μmol·L^{-1}, or 100 μmol·L^{-1} oATP at 37°C for 1 h followed by ATP for 5 min. YO-PRO 1 fluorescence was monitored in a 96-well plate reader using an excitation wavelength of 485 nm, and an emission wavelength of 520 nm. Data are expressed as % of maximum uptake of ATP in the presence of the vehicle. Statistical analyses were performed using one-way ANOVA with Bonferroni *post hoc* test. *P < 0.05 versus control. n = 3. oATP, adenosine 5′-triphosphate, periodate oxidized, sodium salt; YO-PRO 1, quinolinium 4-[(3-methyl-2(3H)-benzoxazolylidene)methyl]-1-[3-(trimethylammonio) propyl]-diiodide.

Table 2 EC_{50} values (μmol·L^{-1} ± SD) for ATP and DBzATP in the absence or presence of the highest concentration of the antagonists in MG63 and SaOS2 cells

	MG63[a]	*SaOS2*[a]
ATP	280 ± 100	290 ± 40
ATP + BBG 5 μmol·L^{-1}	280 ± 100	290 ± 40
ATP	170 ± 50	190 ± 10
ATP + KN-62 10 μmol·L^{-1}	130 ± 10	160 ± 90
ATP	180 ± 10	290 ± 120
ATP + oATP 100 μmol·L^{-1}	120 ± 500	110 ± 90
ATP	260 ± 10	170 ± 80
ATP + PPADS 0.3 μmol·L^{-1}	160 ± 40	150 ± 10
DBzATP	ND	340 ± 150
DBzATP + BBG 5 μmol·L^{-1}	ND	440 ± 150
DBzATP	ND	260 ± 30
DBzATP + KN-62 10 μmol·L^{-1}	ND	230 ± 30

[a]MG63 or SaOS2 cells (approximately 100 000 cells per well) were incubated with 1 μmol·L^{-1} YO-PRO 1 in assay buffer in the presence of water or DMSO (vehicle), or BBG, KN-62, oATP or PPADS at 37°C for 1 h followed by ATP or DBzATP for 5 min. YO-PRO 1 fluorescence was monitored in a 96-well plate reader using an excitation wavelength of 485 nm, and an emission wavelength of 520 nm. EC_{50} values (μmol·L^{-1} ± SD) were calculated using Prism. The data for the highest antagonist concentrations used are shown here. No differences were seen with any of the lower concentrations. n = 3–4.
BBG, brilliant blue G; DBzATP, 2′-3′-O-(4-benzoylbenzoyl)adenosine 5′-triphosphate; KN-62, 4-[(2S)-2-[(5-isoquinolinylsulphonyl)methylamino]-3-oxo-3-(4-phenyl-1-piperazinyl)propyl] phenyl isoquinolinesulphonic acid ester; ND, not determined; oATP, adenosine 5′-triphosphate, periodate oxidized, sodium salt; PPADS, pyridoxal phosphate-6-azo(benzene-2,4-disulphonic acid) tetrasodium salt; YO-PRO 1, quinolinium 4-[(3-methyl-2(3H)-benzoxazolylidene)methyl]-1-[3-(trimethylammonio) propyl]-diiodide.

form of the receptor, and that the 68 kDa form was the deglycosylated receptor. However, after deglycosylation, the mass of the 68 kDa band was reduced by approximately 8 kDa and the 89 kDa band was not seen in these membrane samples suggesting that it is not found in large quantities at the cell surface. Our results therefore suggest that the 68 kDa band represents the functional form of the receptor in human osteoblasts (as it is the glycosylated form) and that the functional form may differ from one cell type to another. Other studies have also suggested this smaller form of the receptor to be the full-length protein (Lee *et al.*, 2006b). The 89 kDa band might represent the extra protein needed for pore formation according to a hypothesis suggested earlier (North, 2002; Faria *et al.*, 2005; Liang and Schwiebert, 2005). An alternative explanation for this 89 kDa band might be that it is a $P2X_4/P2X_7$ receptor heteromer. The possibility of such heteromeric receptors was suggested in a recent study (Guo *et al.*, 2007). We therefore investigated whether $P2X_4/P2X_7$ heteromeric receptors could be detected in MG63 or SaOS2 cells. However, using co-immunoprecipitation techniques, we were unable to find any evidence for the existence of $P2X_4/P2X_7$ heteromeric receptors. Our results suggest that these heteromers are likely to be cell-type-dependent. The most likely explanation therefore for the 89 kDa band seen in this study is that it is an intracellular form of the $P2X_7$ receptor.

We found that the $P2X_7$ receptor was expressed in all the samples used (membranes, nuclei and cell lysates) from both the MG63 and SaOS2 cell lines. Expression levels of $P2X_7$ receptors in both cell lines were similar (data not shown). Results from the immunocytochemistry also showed strong expression in nuclei in both cell lines, mirroring results in THP1 cells (Kidd, unpublished data) and guinea pig smooth muscle cells (Menzies *et al.*, 2003). The specificity of the labelling in the immunocytochemistry was demonstrated by the abolition of staining in cells following pre-adsorption of the primary antibody with its corresponding peptide. The reason for the strong expression of the $P2X_7$ receptor in the nuclei is not clear. It could be related to calcium transport into the nucleus, especially as the intracellular ATP concentration is sufficient to activate the receptor.

We could not detect $P2X_2$ receptor protein in either MG63 or SaOS2 cells in agreement with the lack of detectable mRNA. The $P2X_2$ receptor antibody successfully detected a band in

the positive control which was abolished by pre-adsorption with the corresponding peptide thus confirming the validity of our results.

Once we had shown that MG63 and SaOS2 cells expressed two pore-forming receptors, YO-PRO 1 uptake was studied in both cell lines to determine which receptor was responsible for pore formation.

Different agonists were used to compare their potency at the $P2X_4$ and $P2X_7$ receptors. The results showed that all the agonists were equipotent in inducing YO-PRO 1 uptake with high EC_{50} values in the millimolar range. DBzATP was not more potent than ATP, in contrast to results obtained with transfected receptors (Chessell *et al.*, 1998; Michel *et al.*, 1999; Lee *et al.*, 2006a). However, other studies in cells expressing native $P2X_7$ receptors have either found DBzATP to be equipotent to ATP (Hickman *et al.*, 1994; Coutinho-Silva *et al.*, 1999; Gartland *et al.*, 2001) or to be inactive when used at concentrations up to 100 $\mu mol \cdot L^{-1}$ (Cario-Toumaniantz *et al.*, 1998). Therefore, it is possible that ATP and DBzATP are equipotent in cells expressing endogenous $P2X_7$ receptors and/or that the high receptor number in transfected cells affects the potency of DBzATP.

In a previous study on osteoblasts, Gartland *et al.* (2001) found that a 1 h incubation with agonists was needed for pore formation. In contrast, in our study, a 5 min incubation period was found to give maximal pore formation. This discrepancy might be due to methodological differences in the buffer and dye used (ethidium bromide used by Gartland *et al.*, 2001). Based on the 1 h incubation period needed for pore formation, Gartland *et al.* (2001) suggested that $P2X_7$ receptors have an atypical pharmacology in osteoblasts. We also believe that $P2X_7$ receptors have an atypical pharmacology in osteoblast-like cells but our data are based on the low potency of DBzATP compared with ATP.

Comparison of agonist potencies for our data with those for recombinant $P2X_2$, $P2X_4$ and $P2X_7$ receptors suggested that pore formation in this study is mediated by $P2X_7$ receptors. This is consistent with the results from the RT-PCR and Western blotting for the $P2X_2$ receptor. Although $P2X_4$ receptors are expressed in these cells, these results suggest that they do not contribute significantly to pore formation. The absence of demonstrable receptor desensitization provides further confirmation for the lack of involvement of $P2X_4$ receptors in pore formation in osteoblast-like cells. $P2X_2$ and $P2X_4$ receptors, unlike $P2X_7$ receptors, desensitize upon long exposure to agonists (North and Barnard, 1997; North, 2002; Fountain and North, 2006; Sperlagh *et al.*, 2006).

Further evidence for the involvement of $P2X_7$ rather than $P2X_4$ receptors in pore formation was provided with ivermectin. It is a positive allosteric modulator of $P2X_4$ receptors and used to distinguish current carried by $P2X_4$ receptors from that induced by $P2X_2$, $P2X_3$ or $P2X_7$ receptor stimulation (North, 2002; Gever *et al.*, 2006). The lack of effect of ivermectin on YO-PRO 1 uptake induced by ATP and DBzATP suggests that this uptake is mainly due to $P2X_7$ receptor activation. However, it should be noted that previous studies with ivermectin have only been performed on the $P2X_4$ receptor channel and not the pore (Lalo *et al.*, 2007; Zhang *et al.*, 2007); Emmett *et al.*, 2008), so these results cannot be taken as definitive proof for lack of involvement of the $P2X_4$ receptor.

Interestingly, ATP and 2-Me-S-ATP, at concentrations higher than 1 $mmol \cdot L^{-1}$, were found to reduce YO-PRO 1 uptake, an effect also observed on inducing ethidium uptake by ATP in HEK7 cells (Humphreys *et al.*, 1998; Lee *et al.*, 2006a). This may be due to these agonists binding to the calcium in the buffer (Dweck *et al.*, 2005; Saris and Carafoli, 2005) thus reducing the effective concentration. Another, more likely explanation, given the low concentration of calcium used in the current study, is that concentrations higher than 1 $mmol \cdot L^{-1}$ lead to dephosphorylation of the $P2X_7$ receptor on tyrosine-343. This was seen after repeated application of 100 $\mu mol \cdot L^{-1}$ DBzATP on rat $P2X_7$ receptors where a decline in current recorded was observed (Kim *et al.*, 2001). This dephosphorylation might cause either a change in channel conformation, or disrupt the protein-protein interactions needed for pore formation. Receptor desensitization can be ruled out as an explanation as no evidence was obtained for it here and it has not been reported by other studies.

We tested a number of P2X receptor antagonists to see whether they could block ATP- and DBzATP-induced YO-PRO 1 uptake. Concentration-effect curves for the agonists in the presence of different concentrations of the antagonists were studied. The concentration-effect curves showed that the main action of the antagonists, BBG, KN-62 and PPADS, was to produce a small reduction in the maximum YO-PRO 1 uptake induced by ATP. There was no shift in the EC_{50} values for either agonist with any of the antagonists. oATP had no effect on ATP-induced YO-PRO 1 uptake. We observed that the effect of the antagonists differed between the MG63 and SaOS2 cell lines. The most likely explanation for this finding is the different level of differentiation of these two cell lines (Arnett and Henderson, 1998).

Initial experiments were performed to determine the best pre-incubation period for the antagonists to inhibit YO-PRO 1 uptake and 1 h was found to be the best pre-incubation time (data not shown). The pre-incubation period of P2X receptor antagonists is quite variable between studies. A 30 min pre-incubation period with PPADS, oATP or KN-62 was found to be sufficient to study the antagonist effect of these compounds on DBzATP-induced YO-PRO 1 uptake in HEK7 cells (Michel *et al.*, 2000). This study also reported that 60 min pre-incubation did not increase the antagonist effect of these compounds (Michel *et al.*, 2000). Another study used a 20 min pre-incubation period for KN-62 against DBzATP-induced YO-PRO 1 uptake (White *et al.*, 2005). In human osteoblasts a pre-incubation period of 60 min with PPADS was used to block DBzATP-induced blebbing (Gartland *et al.*, 2001).

The non-competitive inhibition seen with BBG, KN-62 and PPADS in MG63 and SaOS2 cells is similar to data reported in the literature for other cell lines (Michel *et al.*, 2000). BBG has been reported to be more potent at $P2X_7$ receptors compared with the other receptors with an IC_{50} value in the nanomolar range (Hibell *et al.*, 2000; Jiang *et al.*, 2000; Khakh *et al.*, 2001b; Sperlagh *et al.*, 2006). Thus, the inhibition seen here supports the hypothesis that the $P2X_7$ receptor is responsible for pore formation. KN-62 is reported to be the most potent $P2X_7$ receptor antagonist with a nanomolar IC_{50} value (Sperlagh *et al.*, 2006). However, it was not the most potent antagonist in this study. The reason for this difference is not clear,

but may be related to the atypical pharmacology of the $P2X_7$ receptor in human osteoblast-like cells. This is supported by the lack of effect of oATP, another $P2X_7$ receptor antagonist (Michel *et al*., 2000; Gever *et al*., 2006). Another explanation for these results may be the involvement of the $P2X_4$ receptor in pore formation, but this is unlikely as discussed above for a variety of reasons. Furthermore, PPADS, which also had a small inhibitory effect on YO-PRO 1 uptake, is reported to be approximately 10-fold more potent at $P2X_4$ receptors compared with $P2X_7$ receptors (Khakh *et al*., 2001b).

The results presented in this study confirm the expression of the $P2X_7$ receptor in the human osteoblast-like cell lines, MG63 and SaOS2, at the protein and mRNA level. Furthermore, the expression of $P2X_4$ receptor mRNA has been confirmed and the first evidence for the expression of the receptor protein in these cell lines has been obtained. However, heteropolymerization of the $P2X_4$ and $P2X_7$ receptors appears very unlikely in these cell lines. Taken together our results suggest that it is the $P2X_7$ receptor which is responsible for YO-PRO 1 uptake in these two osteoblast-like cell lines. The weak potency of the agonists and the lack of effect of desensitization or ivermectin all militate against an involvement of the $P2X_4$ receptor. The unexpectedly low affinity of DBzATP and the weak action of the antagonists provide further evidence for the atypical pharmacology of the $P2X_7$ receptor in osteoblast cells. Expression of $P2X_7$ receptors in osteoblasts has interesting pathophysiological implications as they are involved in cytokine release and cell death in many cell types. Therefore, they could be involved in conditions such as osteoporosis and rheumatoid arthritis.

Acknowledgements

SM Alqallaf was funded by the Kingdom of Bahrain. We gratefully acknowledge Mrs Carole Elford for technical assistance and Dr Jack Ham for the gift of BON-1 cells.

Conflicts of interest

None.

References

Arnett TR, Henderson B (eds) (1998). *Methods in Bone Biology*. Chapman and Hall: London.

Alexander SPH, Mathie A, Peters JA (2008). Guide to Receptors and Channels (GRAC), 3rd edn. *Br J Pharmacol* **153** (Suppl. 2): S1–S209.

Bianchi BR, Lynch KJ, Touma E, Niforatos W, Burgard EC, Alexander KM *et al*. (1999). Pharmacological characterization of recombinant human and rat P2X receptor subtypes. *Eur J Pharmacol* **376**: 127–138.

Bulanova E, Budagian V, Orinska Z, Hein M, Petersen F, Thon L *et al*. (2005). Extracellular ATP induces cytokine expression and apoptosis through $P2X_7$ receptor in murine mast cells. *J Immunol* **174**: 3880–3890.

Cario-Toumaniantz C, Loirand G, Ferrier L, Pacaud P (1998). Non-genomic inhibition of human $P2X_7$ purinoceptor by 17β-oestradiol. *J Physiol* **508**: 659–666.

Chessell IP, Michel AD, Humphrey PPA (1997). Properties of the pore-forming P2X7 purinoceptor in mouse NTW8 microglial cells. *Br J Pharmacol* **121**: 1429–1437.

Chessell IP, Michel AD, Humphrey PPA (1998). Effects of antagonists at the human recombinant $P2X_7$ receptor. *Br J Pharmacol* **124**: 1314–1320.

Chiozzi P, Sanz JM, Ferrari D, Falzoni S, Aleotti A, Buell GN *et al*. (1997). Spontaneous cell fusion in macrophage cultures expressing high levels of the P2Z/P2X7 receptor. *J Cell Biol* **138**: 697–706.

Collo G, Neidhart S, Kawashima E, Kosco-Vilbois M, North RA, Buell G (1997). Tissue distribution of the P2X7 receptor. *Neuropharmacol* **36**: 1277–1283.

Coutinho-Silva R, Persechini PM, Bisaggio RDC, Perfettini J-L, Neto AC, Kanellopoulos JM *et al*. (1999). P2Z/$P2X_7$ receptor-dependent apoptosis of dendritic cells. *Am J Physiol* **276**: C1139–C1147.

Coutinho-Silva R, Stahl L, Cheung K-K, de Campos NE, de Oliveira Souza C, Ojcius DM *et al*. (2005). P2X and P2Y purinergic receptors on human intestinal epithelial carcinoma cells: effects of extracellular nucleotides on apoptosis and cell proliferation. *Am J Physiol Gastrointest Liver Physiol* **288**: G1024–1035.

Deuchars SA, Atkinson L, Brooke RE, Musa H, Milligan CJ, Batten TFC *et al*. (2001). Neuronal $P2X_7$ receptors are targeted to presynaptic terminals in the central and peripheral nervous systems. *J Neurosci* **21**: 7143–7152.

Di Virgilio F, Chiozzi P, Falzoni S, Ferrari D, Sanz JM, Venketaraman V *et al*. (1998). Cytolytic P2X purinoceptors. *Cell Death Differ* **5**: 191–199.

Di Virgilio F, Chiozzi P, Ferrari D, Falzoni S, Sanz JM, Morelli A *et al*. (2001). Nucleotide receptors: an emerging family of regulatory molecules in blood cells. *Blood* **97**: 587–600.

Dweck D, Reyes-Alfonso JA, Potter JD (2005). Expanding the range of free calcium regulation in biological solutions. *Anal Biochem* **347**: 303–315.

Elliott J, McVey J, Higgins C (2005). The $P2X_7$ receptor is a candidate product of murine and human lupus susceptibility loci: a hypothesis and comparison of murine allelic products. *Arthritis Res Ther* **7**: R468–R475.

Emmett DS, Feranchak A, Kilic G, Puljak L, Miller B, Dolovcak S *et al*. (2008). Characterization of ionotrophic purinergic receptors in hepatocytes. *Hepatology* **47**: 698–705.

Faria RX, DeFarias FP, Alves LA (2005). Are second messengers crucial for opening the pore associated with $P2X_7$ receptor? *Am J Physiol Cell Physiol* **288**: C260–C271.

Ferrari D, Chiozzi P, Falzoni S, Hanau S, Di Virgilio F (1997). Purinergic modulation of interleukin-1β release from microglial cells stimulated with bacterial endotoxin. *J Exp Med* **185**: 579–582.

Fountain SJ, North RA (2006). A C-terminal lysine that controls human $P2X_4$ receptor desensitization. *J Biol Chem* **281**: 15044–15049.

Gartland A, Hipskind RA, Gallagher JA, Bowler WB (2001). Expression of a $P2X_7$ receptor by a subpopulation of human osteoblasts. *J Bone Min Res* **16**: 846–856.

Gartland A, Buckley KA, Bowler WB, Gallagher JA (2003). Blockade of the pore-forming $P2X_7$ receptor inhibits formation of multinucleated human osteoclasts in vitro. *Calc Tissue Int* **73**: 361–369.

Gever JR, Cockayne DA, Dillon MP, Burnstock G, Ford AP (2006). Pharmacology of P2X channels. *Pflügers Arch Eur J Physiol* **452**: 513–537.

Guo C, Masin M, Qureshi OS, Murrell-Lagnado RD (2007). Evidence for functional $P2X_4$/P2X7 heteromeric receptors. *Mol Pharmacol* **72**: 1447–1456.

Hibell AD, Kidd EJ, Chessell IP, Humphrey PPA, Michel AD (2000). Apparent species differences in the kinetic properties of $P2X_7$ receptors. *Br J Pharmacol* **130**: 167–173.

Hickman SE, el Khoury J, Greenberg S, Schieren I, Silverstein SC (1994). P2Z adenosine triphosphate receptor activity in cultured human monocyte-derived macrophages. *Blood* **84**: 2452–2456.

Hoebertz A, Townsend-Nicholson A, Glass R, Burnstock G, Arnett TR (2000). Expression of P2 receptors in bone and cultured bone cells. *Bone* **27**: 503–510.

Hoebertz A, Arnett TR, Burnstock G (2003). Regulation of bone resorption and formation by purines and pyrimidines. *Trends Pharmacol Sci* **24**: 290–297.

Hughes FJ, Aubin JE (1998). Culture of cells of the osteoblast lineage. In: Arnett TR, Henderson, B (eds). *Methods in Bone Biology*. Chapman and Hall: London, pp. 1–49.

Humphreys BD, Virginio C, Surprenant A, Rice J, Dubyak GR (1998). Isoquinolines as antagonists of the P2X$_7$ nucleotide receptor: high selectivity for the human versus rat receptor homologues. *Mol Pharmacol* **54**: 22–32.

Jiang LH, Mackenzie AB, North RA, Suprenant A (2000). Brilliant Blue G selectively blocks ATP-gated rat P2X$_7$ receptors. *Mol Pharmacol* **58**: 82–88.

Jorgensen NR, Henriksen Z, Sorensen OH, Eriksen EF, Civitelli R, Steinberg TH (2002). Intercellular calcium signalling occurs between human osteoblasts and osteoclasts and requires activation of osteoclast P2X$_7$ receptors. *J Biol Chem* **277**: 7574–7580.

Ke HZ, Qi H, Weidema AF, Zhang Q, Panupinthu N, Crawford DT *et al*. (2003). Deletion of the P2X$_7$ nucleotide receptor reveals its regulatory roles in bone formation and resorption. *Mol Endocrinol* **17**: 1356–1367.

Khakh BS (2001a). Molecular physiology of P2X receptors and ATP signalling at synapses. *Nature RevNeurosci* **2**: 165–174.

Khakh BS, Burnstock G, Kennedy C, King BF, North RA, Seguela P *et al*. (2001b). International Union of Pharmacology.XXIV. Current status of the nomenclature and properties of P2X receptors and their subunits. *Pharmacol Rev* **53**: 107–118.

Kim M, Jiang LH, Wilson HL, North RA, Surprenant A (2001). Proteomic and functional evidence for a P2X$_7$ receptor signalling complex. *EMBO J* **20**: 6347–6358.

Kobayashi K, Fukuoka T, Yamanaka H, Dai Y, Obata K, Tokunaga A *et al*. (2005). Differential expression patterns of mRNAs for P2X receptor subunits in neurochemically characterized dorsal root ganglion neurons in the rat. *J Comp Neurol* **481**: 377–390.

Labasi JM, Petrushova N, Donova C, McCurdy S, Lira P, Payette MM *et al*. (2002). Absence of the P2X$_7$ receptor alters leukocyte function and attenuates an inflammatory response. *J Immunol* **168**: 6436–6445.

Lalo U, Verkhratsky A, Pankratov Y (2007). Ivermectin potentiates ATP-induced ion currents in cortical neurones: Evidence for functional expression of P2X4 receptors? *Neurosci Lett* **421**: 158–162.

Lee SY, Jo S, Lee GE, Jeong LS, Kim YC, Park CS (2006a). Establishment of an assay for P2X$_7$ receptor-mediated cell death. *Mol Cells* **22**: 198–202.

Lee DH, Park KS, Kong ID, Kim JW, Han BG (2006b). Expression of P2 receptors in human B cells and Epstein-Barr virus-transformed lymphoblastoid cell lines. *BMC Immunol* **7**: 22.

Liang L, Schwiebert EM (2005). Large pore formation uniquely associated with P2X7 purinergic receptor channels. Focus on 'Are second messengers crucial for opening the pore associated with P2X7 receptor?' *Am J Physiol Cell Physiol* **288**: C240–C242.

Lynch KJ, Touma E, Niforatos W, Kage KL, Burgard EC, Van Biesen T *et al*. (1999). Molecular and functional characterization of human P2X2 receptors. *Mol Pharmacol* **56**: 1171–1181.

Menzies J, Paul A, Kennedy C (2003). P2X$_7$ subunit-like immunoreactivity in the nucleus of visceral smooth muscle cells of the guinea pig. *Auton Neurosci* **106**: 103–109.

Michel AD, Chessell IP, Humphrey PPA (1999). Ionic effects on human recombinant P2X$_7$ receptor function. Naunyn-Schmied. *Arch Pharmacol* **359**: 102–109.

Michel AD, Kaur R, Chessell IP, Humphrey PPA (2000). Antagonist effects on human P2X$_7$ receptor-mediated cellular accumulation of YO-PRO-1. *Br J Pharmacol* **130**: 513–520.

Naemsch LN, Dixon SJ, Sims SM (2001). Activity-dependent development of P2X$_7$ current and Ca^{2+} entry in rabbit osteoclasts. *J Biol Chem* **276**: 39107–39114.

Nakamura E, Uezono Y, Narusawa K, Shibuya I, Oishi Y, Tanaka M *et al*. (2000). ATP activates DNA synthesis by acting on P2X receptors in human osteoblast-like MG-63 cells. *Am J Physiol Cell Physiol* **279**: C510–C519.

North RA (2002). Molecular physiology of P2X receptors. *Physiol Rev* **82**: 1013–1067.

North RA, Barnard E (1997). Nucleotide receptors. *Curr Opin Neurobiol* **7**: 346–357.

Saris N-EL, Carafoli E (2005). A historical review of cellular calcium handling, with emphasis on mitochondria. *Biochem* **70**: 187–194.

Sluyter R, Wiley JS (2002). Extracellular adenosine 5′-triphosphate induces a loss of CD23 from human dendritic cells via activation of P2X$_7$ receptors. *Int Immunol* **14**: 1415–1421.

Solle M, Labasi J, Perregaux DG, Stam E, Petrushova N, Koller BH *et al*. (2001). Altered cytokine production in mice lacking P2X$_7$ receptors. *J Biol Chem* **276**: 125–132.

Sperlagh B, Vizi ES, Wirkner K, Illes P (2006). P2X$_7$ receptors in the nervous system. *Prog Neurobiol* **78**: 327–346.

Steinberg T, Newman A, Swanson J, Silverstein S (1987). ATP4- permeabilizes the plasma membrane of mouse macrophages to fluorescent dyes. *J Biol Chem* **262**: 8884–8888.

Suprenant A, Rassendren F, Kawashima E, North RA, Buell G (1996). The cytoloytic P$_{2z}$ receptor for extracellular ATP identified as a P$_{2x}$ receptor (P2X$_7$). *Science* **272**: 735–738.

Thomas RS, Liddell JE, Murphy LS, Pache DM, Kidd EJ (2006). An antibody to the β-secretase cleavage site on amyloid-β-protein precursor inhibits amyloid-β production. *J Alzheimers Dis* **10**: 379–390.

Thunberg U, Tobin G, Johnson A, Soderberg O, Padyukov L, Hultdin M *et al*. (2002). Polymorphism in the P2X$_7$ receptor gene and survival in chronic lymphocytic leukaemia. *Lancet* **360**: 1935–1939.

Vial C, Roberts JA, Evans RJ (2004). Molecular properties of ATP-gated P2X receptor ion channels. *Trends Pharmacol Sci* **25**: 487–493.

Virginio C, MacKenzie A, Rassendren FA, North RA, Surprenant A (1999). Pore dilation of neuronal P2X receptor channels. *Nature Neurosci* **2**: 315–321.

Wang Q, Li X, Wang L, Feng Y-H, Zeng R, Gorodeski G (2004a). Antiapoptotic effects of estrogen in normal and cancer human cervical epithelial cells. *Endocrinology* **145**: 5568–5579.

Wang Q, Wang L, Feng Y-H, Li X, Zeng R, Gorodeski GI (2004b). P2X$_7$ receptor-mediated apoptosis of human cervical epithelial cells. *Am J Physiol Cell Physiol* **287**: C1349–C1358.

Wang L, Feng Y-H, Gorodeski GI (2005). Epidermal growth factor facilitates epinephrine inhibition of P2X$_7$-receptor-mediated pore formation and apoptosis: a novel signaling network. *Endocrinol* **146**: 164–174.

White N, Butler PEM, Burnstock G (2005). Human melanomas express functional P2X$_7$ receptors. *Cell Tissue Res* **321**: 411–418.

Wiley JS, Dao-Ung LP, Gu BJ, Sluyter R, Shemon AN, Li C *et al*. (2002). A loss-of-function polymorphic mutation in the cytolytic P2X$_7$ receptor gene and chronic lymphocytic leukaemia: a molecular study. *Lancet* **359**: 1114–1119.

Wilson HL, Francis SE, Dower SK, Crossman DC (2004). Secretion of intracellular IL-1 receptor antagonist (Type 1) is dependent on P2X$_7$ receptor activation. *J Immunol* **173**: 1202–1208.

Yates L, Clark JH, Martin TJ, James S, Broadley KJ, Kidd EJ (2006). Radioligand binding and functional responses of ligands for human recombinant adenosine A$_3$ receptors. *Auton Autacoid Pharmacol* **26**: 191–200.

Zhang X, Zheng G, Ma X, Yan Y, Li G, Rao Q *et al*. (2004). Expression of P2X$_7$ in human hematopoietic cell lines and leukemia patients. *Leuk Res* **28**: 1313–1322.

Zhang Y, Sanchez D, Gorelik J, Klenerman D, Lab M, Edwards C *et al*. (2007). Basolateral P2X$_4$-like receptors regulate the extracellular ATP-stimulated epithelial Na+ channel activity in renal epithelia. *Am J Physiol Renal Physiol* **292**: F1734–1740.